Mode softening, precursor phenomena, and intermediate phases in $PbZrO_3$

Jae-Hyeon Ko,[1] Michał Górny,[2] Andrzej Majchrowski,[3] Krystian Roleder,[2] and Annette Bussmann-Holder[4]
[1]*Department of Physics, Hallym University, 39 Hallymdaehakgil, Chuncheon, Gangwondo 200-702, Korea*
[2]*Institute of Physics, University of Silesia, ulica Uniwersytecka 4, PL-40-007 Katowice, Poland*
[3]*Institute of Applied Physics, Military University of Technology, ul. Kaliskiego 2, 00-908 Warsaw, Poland*
[4]*Max-Planck-Institut für Festkörperforschung, Heisenbergstr. 1, D-70569 Stuttgart, Germany*
(Received 24 January 2013; revised manuscript received 8 April 2013; published 14 May 2013)

Single crystals of $PbZrO_3$ have been studied by Brillouin light scattering, birefringence, and piezoelectric coefficient measurements. The structural phase transition at T_c is shown to be related to the softening of a longitudinal acoustic (LA) mode, whereas precursor effects are deduced from a central peak in the light scattering spectrum, finite birefringence, and piezoelectric coefficient above the structural instability. An intermediate phase in the vicinity of T_c is apparent where a coexistence of the LA mode with a high frequency mode appears, and in addition the transverse acoustic (TA) mode becomes visible.

DOI: 10.1103/PhysRevB.87.184110 PACS number(s): 77.80.−e, 77.84.−s, 78.35.+c

I. INTRODUCTION

$PbZrO_3$(PZO) is one of the end members of famous piezoelectric $PbZr_{1-x}Ti_xO_3$ (PZT) complex perovskites and is known as the first compound confirmed to have antiferroelectricity.[1] The phase transition of $PbZrO_3$ has been a matter of intensive investigations since its discovery.[2] While the observation of a dielectric anomaly has first been thought to be related to a ferroelectric instability,[3] a subsequent study arrives at the conclusion that the compound must be antiferroelectric,[4] however, without knowing its origin. A first detailed x-ray and neutron diffraction study[5] clarified the low temperature structure and assigned it to the space group *Pba2*, but a more recent diffractions study found that the room-temperature structure is nonpolar *Pbam*.[6] The antiferroelectric properties arise from antiparallel shifts of the Pb atoms in the (110) plane.[6] In addition the oxygen atoms undergo antiparallel shifts within the (001) plane and along the *c* axis. These latter displacements have been speculated to be responsible for an intermediate, ferroelectric phase within a few degrees below T_c,[7–11] the existence of which was also confirmed by subsequent studies.[12–16] It was found that the observation of ferroelectricity was closely related to defects or stoichiometrical deviations.[12,13]

A detailed structural analysis arrived at the conclusion that two phenomena take place at T_c simultaneously, namely Pb ion displacements, giving rise to antiferroelectricity, and ZrO_6 octahedral tilts.[12] Lattice dynamic calculations showed that both Γ point and *R* point instabilities coexist in PZO.[17] These combined structural anomalies have been interpreted in terms of coupled order parameters[18] and speculated to be connected with the condensation of a normal mode. Very recently, Tagantsev *et al*. suggested that phonon instability occurred at the Γ point, but not at *R* or other points in the first Brillouin zone of PZO based on their inelastic and diffuse x-ray scattering study.[19] The substitution of Zr cations by a small amount of Ti cations normally induces a rhombohedral ferroelectric phase in the PZT phase diagram, which indicates that the energy difference between the antiferroelectric structure and the ferroelectric one is very small. Indeed, it was found by total energy calculations that the structure of PZO is unstable against both antiferroelectric and ferroelectric distortions, implying a delicate balance between these two competing instabilities.[17,20,21] This may be one of the reasons why weak field-induced ferroelectricity could be observed even in the antiferroelectric phase of PZO ceramics.[22]

In relation to the antiferroelectric phase transition of PZO, its precursor phenomena in the high-temperature cubic phase have attracted attention from the viewpoint of the nature of the phase transition. The observation of first-order Raman spectrum and piezoelectric effect in the paraelectric phase of PZO suggested the existence of polar regions with broken symmetry.[23,24] In addition, a polar relaxation mode was observed in either the microwave or terahertz frequency range.[25,26] These dielectric dispersions were attributed to the anharmonic motions of Pb ions in the lattice and discussed in the framework of the order-disorder mechanism.[25] The disordering of the Pb atoms in the paraelectric phase was also confirmed by the high-energy x-ray powder diffraction measurements and attributed to the electron hybridization between O and the disordered Pb in the cubic phase.[27] However, more detailed lattice dynamical studies on PZO should be carried out to reveal the origin of the antiferroelectric phase transition and its relation to the precursor phenomena, which have been difficult to perform due to the lack of high-quality single crystals.

The purpose of this paper is to explore the precursor phenomena and the nature of the intermediate phase of PZO single crystals by Brillouin light scattering, birefringence, and piezoelectric coefficient measurements. We applied the Brillouin scattering technique to study long-wavelength acoustic modes and elastic properties of PZO near the center of the first Brillouin zone. The existence of precursor polar clusters with broken symmetry in the paraelectric phase will be discussed in relation to the antiferroelectric phase transition of PZO.

II. EXPERIMENT

Lead zirconate single crystals were grown from high temperature solutions (flux growth method) by means of spontaneous crystallization. A one-zone resistance furnace was controlled with the Eurotherm 2704 microprocessor regulator. A Pb_3O_4-B_2O_3 mixture was used as the solvent. The composition of the melt used in our experiments was

the same as in Ref. 28: 2.4 mol% of $PbZrO_3$, 77 mol% of PbO (re-counted to Pb_3O_4), and 20.6 mol% of B_2O_3. Pb_3O_4 was used instead of PbO to avoid dark-grey coloration of the as-grown crystals. The total mass of the melt was equal to 140 g. The melt was synthesized directly in a Pt crucible. The crucible covered with a Pt lid was heated up to 1350 K. The temperature, measured under the bottom of the crucible, was kept for at least three hours to enable complete soaking of the melt. Owing to thermal isolation the temperature gradient in the melt was kept around 5 K/cm. After soaking the melt temperature was lowered at a rate of 3.5 K/h down to 1120 K. In the following step the remaining melt was decanted and as-grown crystals attached to the crucible walls were cooled down to the room temperature at a rate of 10 K/h. In the final step the as-grown crystals were etched in diluted acetic acid to remove residues of the solidified flux. An easy evaporation of PbO during crystal growth is mainly responsible for the stoichiometry of lead zirconate crystals. In order to check the stoichiometry, we used a scanning electron microscope, with an energy dispersive x-ray spectrometer (EDS), to determine the Pb and Zr concentrations, which was found to be $50.34 \pm 0.3\%$ and $49.66 \pm 0.3\%$, respectively.

The grown single crystals were transparent and of high optical quality, and cut to have (100) pseudocubic surfaces. A conventional tandem multipass Fabry-Perot interferometer was used to measure the Brillouin spectrum in a narrow (±60 GHz) and a wide (±600 GHz) frequency range by using different free spectral ranges. The sample was inserted in a cryostate (THMS 600, Linkam), which was put on a microscope (BX41, Olympus) for backscattering geometry. A solid state laser (Excelsior 532-300, SpectraPhysics) at a wavelength of 532 nm was used as an excitation source. The details of the Brillouin spectrometer used for this study can be found from Ref. 29. The laser beam was incident on the (100) plane of PZO single crystal, and thus the phonon wave vector was along the [100] direction. The birefringence measurements were performed by means of an Oxford Cryosystems Metripol Birefringence Imaging System (Metripol). The sample was held by a high precision Linkam TMSG600 temperature stage combined with the Metripol. Details of this automated optical technique are described in Ref. 30. The measurement method of the piezoelectric property is described in Ref. 24.

III. RESULTS AND DISCUSSION

Figure 1 shows two Brillouin spectra of PZO, one at 235 °C just above T_c and the other at 234 °C just below T_c. The spectrum above T_c consists of one Brillouin doublet corresponding to the longitudinal acoustic (LA) mode consistent with the Brillouin selection rule of the cubic symmetry.[31] Two remarkable changes occur when the PZO single crystal undergoes a phase transition, i.e., the splitting of the LA mode and the appearance of the transverse acoustic (TA) mode located at around 27 GHz. These changes clearly indicate a structural phase transition occurring in PZO. Figure 1(b) shows the extended view of the Stokes-shifted Brillouin spectra at several temperatures around T_c. The high-temperature, low-frequency LA mode decreases gradually while the new, high-frequency peak grows upon cooling. This apparent intensity

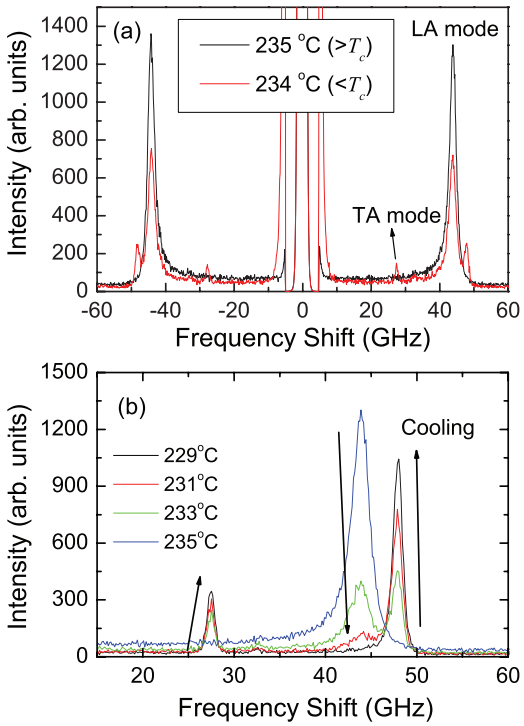

FIG. 1. (Color online) (a) Two Brillouin spectra of PZO, one at 235 °C just above T_c and the other at 234 °C just below T_c. (b) The extended view of the Stokes-shifted Brillouin spectra at several temperatures around T_c.

transfer is completed in a specific temperature range between 234 and 229 °C, which can be regarded as the one where the intermediate phase appears in PZO.

The Brillouin spectra were fitted by using a superposition of response functions of the damped harmonic oscillator, from which the Brillouin frequency shift (ν_B) and the full-width at half-maximum (FWHM, Γ_B) could be obtained. Figures 2(a) and 2(b) show the temperature dependence of ν_B and Γ_B of the LA mode, respectively. ν_B exhibits softening upon cooling in the paraelectric phase, which is accompanied by the increasing hypersonic damping as shown in Fig. 2(b). In principle, the elastic constant C_{11} can be derived from ν_B if the temperature dependencies of both the refractive index at the wavelength of 532 nm and the density are known in the cubic phase. However, these data are not available from previous studies. We roughly estimated the elastic constant of PZO by using a calculated density based on the reported lattice constants at 520 K (7.9826 g/cm^3)[27] and the average refractive index of the orthorhombic phase(∼2.36),[12,32] their temperature dependencies not being considered. This crude calculation showed that C_{11} changes from ∼232 GPa at 400 °C to ∼195 GPa near T_c. These values are systematically larger than the predicted values by first-principles calculations (∼151–161 GPa) in the cubic phase,[17,33] indicating that the effective Hamiltonians used for these calculations should be refined. As the inset of Fig. 2(a) presents, ν_B shows a clear splitting in the intermediate phase. The high-temperature LA mode is substantially damped out as can be seen from the rapid increase in Γ_B [see the inset of Fig. 2(b)], while the newly-emerging LA mode is stabilized in the intermediate

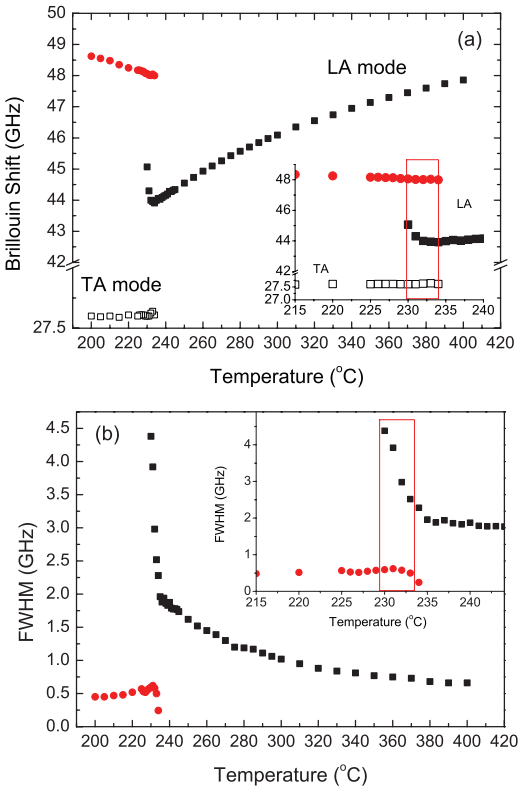

FIG. 2. (Color online) Temperature dependencies of (a) the Brillouin frequency shift and (b) the FWHM of the LA mode. The insets show the extended view of the Brillouin shift (top) and the FWHM (bottom) at temperatures near the intermediate phase. The red boxes in the insets indicate the approximate range of the intermediate phase.

phase and shows continuous evolution into the orthorhombic phase. On the other hand, the TA mode appears at about 234 °C and does not show any anomaly in both the intermediate and the antiferroelectric phases. Brillouin spectrum was measured down to −196 °C, but there was no elastic anomaly in both ν_B and Γ_B indicating that no further low-temperature phase transition exists in PZO. This result is consistent with previous results of elastic moduli of PZO ceramics.[34]

The gradual softening of ν_B along with the increase in Γ_B in the paraelectric phase is also observed from typical ferroelectrics such as $BaTiO_3$ single crystals.[35–37] The precursor polar clusters and their interaction with acoustic waves via electrostrictive coupling were suggested to be the origin which causes these acoustic anomalies. The precursor polar clusters may manifest themselves in the inelastic light scattering spectrum as quasielastic central peaks because of their relaxational motions, which motivated us to investigate the Brillouin spectrum in a much broader frequency range. Figure 3 shows the depolarized Brillouin spectra within ±560 GHz in the paraelectric phase. The frequency scale is expressed in both units, GHz and wave number (1 cm^{-1} = 30 GHz). The quasielastic central peak grows upon cooling in the temperature range between ∼300 °C and T_c. The central peak was fitted by using the single Debye function, and the solid lines in Fig. 3 represent the best-fit results. The half width, which is inversely proportional to the relaxation time,

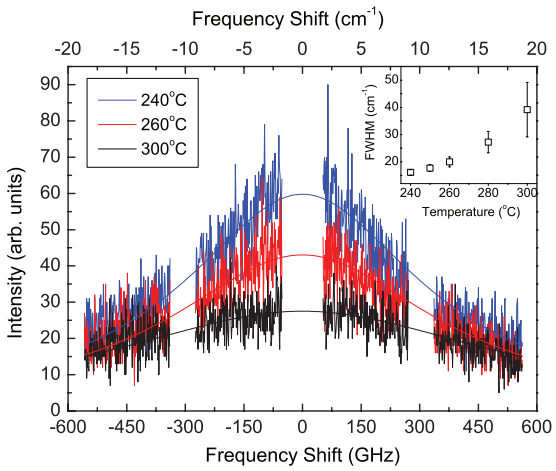

FIG. 3. (Color online) Depolarized Brillouin spectra of PZO in a broad frequency range. Solid lines denote the best-fit results in terms of a single Debye relaxation process. The inset shows the FWHM of the central peak which is inversely proportional to the relaxation time.

is shown in the inset of Fig. 3 in the unit of wave number. The inset exhibits that the relaxation time increases on approaching T_c in the paraelectric phase. This result is consistent with the observation of a central-mode type dispersion observed in the terahertz range studied by infrared (IR) reflectivity measurements,[26] and also a relaxational soft mode at the Γ point studied by the recent inelastic x-ray study.[19] The growing central peak (central mode in Ref. 26) is thus considered to be related to the large dielectric anomaly observed in the paraelectric phase of PZO. However, mainly the LA mode and the corresponding central peak were investigated in this study because of the backscattering geometry. The relevant displacement of the LA mode driven by C_{11} elastic constant is coupled to the square of the order parameter due to its nature of full symmetry in the long-wavelength approximation. This is the origin why the LA mode softening is relatively small and shows a weaker critical behavior as observed in Fig. 2(a). In the same context, the slowing down of the relaxation process presented by the central peak in the light scattering spectrum may not account for the whole dielectric anomaly of PZO in the paraelectric phase. However, both the central peak from this Brillouin scattering study and the central mode from IR study[26] are attributed to the anharmonic Pb hopping motions, and thus the characteristic time scales of both studies are expected to be similar, as is confirmed by comparing the inset of Fig. 3 and Fig. 2 in Ref. 26.

Figure 4(a) shows the temperature dependence of the birefringence (Δn) of the same crystal used for the Brillouin scattering in the paraelectric phase. In principle, Δn should be zero in the centrosymmetric cubic phase. However, it exhibits clear nonzero values in a certain temperature range from T_c to ∼300 °C. This temperature range is almost the same as that where the central peak grows substantially. Figure 4(b) shows the piezoelectric coefficient d_{11} of another PZO single crystal, from the same technological process, in three phases. Although it is very weak, d_{11} shows nonzero values in a similar temperature range in the centrosymmetric paraelectric phase. All these results clearly indicate that local

noncentrosymmetric regions appear in this temperature region, which are responsible for nonzero Δn and d_{11} in addition to the growing central peak. First-principles calculations showed that unstable modes in the Pb subspace may induce a possible local order of polar distortions in a temperature range of 80 °C above T_c.[17] This temperature range is almost the same as that where we observed anomalies in the central peak, Δn, and d_{11}. This result is also consistent with the theoretical predictions by Bussmann-Holder *et al.*, which suggests that precursor dynamics are always present and that this is independent of the shape and the depth of the doublewell potential.[38] According to this prediction, polar clusters are growing rapidly on approaching T_c from the high-temperature side, reaching several lattice constants at $T/T_c = 1.1$. Taking into account the value of T_c equal to 508 K (~235 °C), the temperature window $\Delta T = (1.1 \times T_c) - T_c = (1.1 \times 508) - 508\ \text{K} = 51\ \text{K}$. This points out that rapidly-growing polar clusters will induce anomalous behaviors in the temperature range from T_c to ~289 °C, and all anomalies described in this paper have in fact been observed in this temperature range.

Apparently, the observation of the birefringence in the paraelectric phase does not seem to be compatible with the average cubic symmetry. Existence of polar regions that make the crystal birefringent was also seen in the paraelectric phase of barium titanate.[36] The distribution of polar regions, embedded in the paraelectric matrix, is not homogenous and their sizes and density may differ in different volumes of crystal. Such inhomogeneous distribution was also reported in Ref. 36, where regions of the size of microns have been directly observed. In the investigated PZO single crystals the value of birefringence above T_c was of similar order of magnitude as that of barium titanate. This indicates that the size of polar regions—in spite of the fact that they were not as clearly visible as in barium titanate—in lead zirconate are much smaller, but some are still big enough in comparison of light wavelength to cause the birefringence effect. We thus cannot exclude the possibility that birefringence may be due to some strains and other defects in the crystal. It is known from, for example, high-resolution transmission electron microscopy, that defects, like dislocations and/or shear planes, are present in perovskites.[39,40] Around such lattice faults, which are difficult to remove by thermal rejuvenation, the local mechanical and electrical stresses can be created. These stresses may cause that the structural instability[38] transforms into much larger and strongly pinned polar regions above T_c observed in birefringence experiments. On the other hand, large dynamic polar clusters might also contribute to the weak anomalous behaviors shown in Fig. 4, in particular, the piezoelectric effects. The precursor dynamics of PZO is connected with the disorder in the Pb and O sublattice,[41] and the characteristic time and length scales are expected to become longer near T_c because of their masses, longer hopping times, and enhanced correlations upon approaching the phase transition. That is, although there is no macroscopic symmetry breaking from the static sense, correlated off-centering motions, which induce local symmetry breaking, exist in the paraelectric phase, and some large dynamic clusters might contribute to the very weak anomalous behaviors which we observed in the paraelectric phase. In particular, the piezoelectric response shown in Fig. 4(b) was measured under the applied external electric field

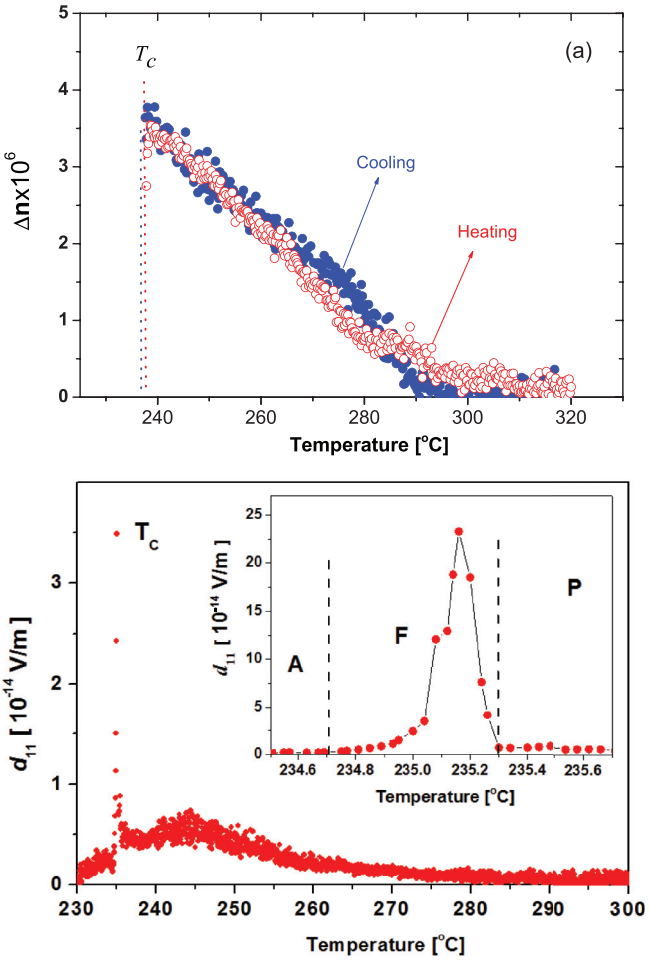

FIG. 4. (Color online) (a) Temperature dependence of the birefringence (Δn) in the paraelectric phase measured at both cooling and heating processes. (b) Temperature dependence of the piezoelectric coefficient d_{11} in three phases measured upon cooling. The inset shows the the extended plot of d_{11} near the intermediate phase.

(see Ref. 24), which is a conjugate field to the polarization, tends to increase the correlation length and lifetime of the polar clusters, and thereby may contribute to the tiny but nonzero piezoelectric response. Clear distinction between these two contributions to the nonzero birefringence and piezo-response in the paraelectric phase could not be made from this study, which requires more elaborate and sophisticated approaches. Study on high-quality PZO single crystals which may not exhibit intermediate phase is desirable from this point of view.

In contrast to the weak values of d_{11} in the paraelectric phase, it exhibits a sharp increase in the intermediate phase as can be seen from the extended plot shown in the inset of Fig. 4(b). This result strongly indicates that the nature of the intermediate phase is ferroelectric. The existence of the intermediate phase was already suggested by Sawaguchi *et al.*[4] by means of polarization-electric field hysteresis measurements in 1951, and then its nature was suggested to be rhombohedral ferroelectric phase by Tennery[7,8] and Goulpeau.[9] Subsequent reports confirmed it by observing a single electric field-polarization hysteresis loop with a large polarization value, pyroelectric current, and ferroelectric domains by transmission electron microscopy.[10,13,14,16] Our

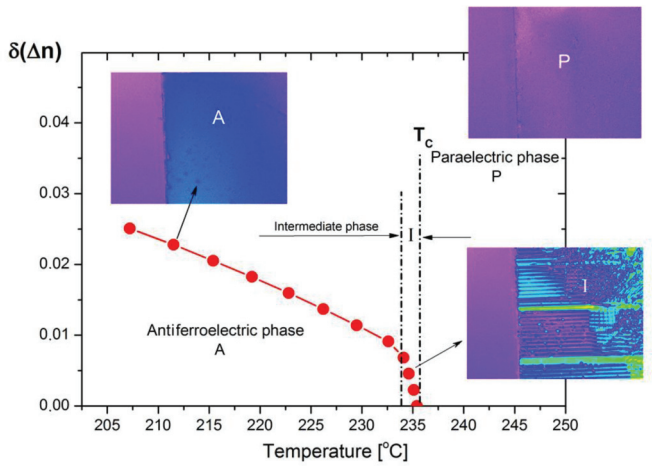

FIG. 5. (Color online) Temperature dependence of the birefringence in the vicinity of phase transitions. A, I and P denote the aniferroelectric, intermediate and paraelectric phase. Insets represent distribution of birefringence in crystals in subsequent phases. Appearance of I phase is seen both on $\delta(\Delta n)(T)$ run as a change of the slope of this function and in the inset showing complex distributions of birefringence corresponding to disordered domains structure. The function $\delta(\Delta n)(T) = \Delta n(T) - \Delta n(T_C)$ has been determined for an area of 135*25 μm^2. Approximate temperature range of the intermediate phase was indicated by two vertical lines.

observation of large piezoelectric coefficient below T_c is thus complementary evidence for the ferroelectric nature of the intermediate phase of PZO. d_{11} becomes very small upon entering into the centrosymmetric antiferroelectric phase from the intermediate one.

The ferroelectric nature and the splitting of the LA mode in the intermediate phase may be understood in the following way. The splitting of the LA mode indicates that the PZO single crystal consists of two domains in the intermediate phase: one has the high-temperature prototype phase and the other has the antiferroelectric orthorhombic phase. Considering the intensity transfer from the high-temperature LA mode peak to the low-temperature one occurring in the intermediate phase, the antiferroelectric domains seem to coexist with the prototype phase, growing gradually upon cooling and to percolate the whole system at the lower bound of the intermediate phase. However, the prototype phase is expected to include many polar clusters since we observed birefringence, central peak, and piezoelectric effect in the paraelectric phase close to T_c. The rapid increase in d_{11} just below T_c seems to indicate a substantial increase in the size of these "ferroelectric" polar clusters in the prototype phase coexisting with antiferroelectric domains. Then, the substantial decrease in d_{11} upon further cooling seems to be a natural result because the antiferroelectric domains, which are centrosymmetric and thus cannot contribute to d_{11}, will grow and percolate the whole volume at the lower bound of the intermediate phase. The coexistence of these two phases can also be clearly seen from Fig. 5, which shows the birefringence data in three phases. Different colors represent different values of birefringence. A pinklike color in the paraelectric phase corresponds to almost a zero value of birefringence. It is clearly seen that, in the intermediate phase, there is a coexistence of different domains, while there is a single domain in the antiferroelecrtic phase. It should be pointed out that the measured value of Δn in the intermediate phase gives an average value due to the tiny domain structure. The coexistence of antiferroelectric domains and ferroelectrically-active regions in the intermediate phase may be justified by the fact that the difference in the total energy between the ferroelectric and antiferroelectric phase is very small as the first-principles calculations already suggested.[17,20,21] Induced or intrinsic defects in the crystal may have effects on the energy configuration and play some role in the appearance of transient ferroelectric phase in PZO.[13] However, a more sophisticated approach is necessary to get detailed insights into the microscopic nature of the intermediate phase of PZO.

IV. CONCLUSION

In conclusion, the present study on PZO single crystals revealed that the structural phase transition at T_c was accompanied by the softening of a LA mode along with increasing hypersonic damping and that precursor polar clusters were formed in the paraelectric phase and grew rapidly upon cooling in a certain temperature range of $\sim$80 °C above T_c as revealed by finite birefringence and piezoelectric coefficient above the structural instability. The precursor effects were also associated with the growing central peak that reflects the relaxational motions of these polar regions. An intermediate phase in the vicinity of T_c was apparent where a coexistence of the LA mode with a high frequency mode appeared and in addition the TA mode became visible. The high piezoresponse observed in the intermediate phase was ascribed to the "ferroelectric" polar regions embedded in the paraelectric matrix coexisting with antiferroelectric domains.

ACKNOWLEDGMENTS

This research was supported by Basic Science Research Program through the National Research Foundation of Korea (NRF) funded by the Ministry of Education, Science and Technology (2010-0010497) and by the National Center for Science (NCN) in Poland within the project 1955/B/H03/2011/40.

[1]H. Liu and B. Dkhil, Z. Kristallogr. **226**, 163 (2011).
[2]S. Roberts, J. Am. Ceram. Soc. **33**, 63 (1950).
[3]G. Shirane, E. Sawaguchi, and Y. Takagi, Phys. Rev. **84**, 476 (1951).
[4]E. Sawaguchi, G. Shirane, and Y. Takagi, J. Phys. Soc. Jpn. **6**, 333 (1951).
[5]F. Jona, G. Shirane, F. Mazzi, and R. Pepinsky, Phys. Rev. **105**, 849 (1957).
[6]D. L. Corker, A. M. Glazer, J. Dec, K. Roleder, and R. W. Whatmore, Acta Cryst. **B53**, 135 (1997).
[7]V. J. Tennery, J. Electrochem. Soc. **112**, 1117 (1965).

[8]V. J. Tennery, J. Am. Ceram. Soc. **49**, 483 (1966).
[9]L. Goulpeau, Sov. Phys. Solid State **8**, 1970 (1967).
[10]B. A. Scott and G. Burns, J. Am. Ceram. Soc. **55**, 331 (1972).
[11]Z. Ujma and J. Handerek, Phys. Stat. Solidi (a) **28**, 489 (1975).
[12]R. W. Whatmore and A. M. Glazer, J. Phys. C: Solid State Phys. **12**, 1505 (1979).
[13]K. Roleder and J. Dec, J. Phys.: Condens. Matter **1**, 1503 (1989).
[14]D. Viehland, Phys. Rev. B **52**, 778 (1995).
[15]A. A. Belov, Y.-H. Jeong, and K. Y. Kang, J. Korean Phys. Soc. **32**, S299 (1998).
[16]P. S. Dobal, R. S. Katiyar, S. S. N. Bharadwaja, and S. B. Krupanidhi, Appl. Phys. Lett. **78**, 1730 (2001).
[17]U. V. Waghmare and K. M. Rabe, Ferroelectrics **194**, 135 (1997).
[18]H. Fujishita, Y. Ishikawa, S. Tanaka, A. Ogawaguchi, and S. Katano, J. Phys. Soc. Jpn. **72**, 1426 (2003).
[19]A. K. Tagantsev, S. B. Vakhrushev, K. Vaideeswaran, A. V. Filimonov, R. G. Burkovsky, A. Shaganov, D. Andronikova, A. I. Rudskoy, A. Q. R. Baron, H. Uchiyama, D. Chernyshov, A. Bosak, Z. Ujima, K. Roleder, and N. Setter, in *Abstract Book of the Fundamental Physics of Ferroelectrics and Related Materials 2013* (Iowa Stat Univ., Ames, 2013), pp. 40–41.
[20]D. J. Singh, Phys. Rev. B **52**, 12559 (1995).
[21]R. Kagimura and D. J. Singh, Phys. Rev. B **77**, 104113 (2008).
[22]X. Dai, J.-F. Li, and D. Viehland, Phys. Rev. B **51**, 2651 (1995).
[23]G. Kugel, I. Jankowska-Sumara, K. Roleder, and J. Dec, J. Korean Phys. Soc. **32**, S581 (1998).
[24]K. Wieczorek, A. Ziebińska, Z. Ujma, K. Szot, M. Górny, I. Franke, J. Koperski, A. Soszyński, and K. Roleder, Ferroelectrics **336**, 61 (2008).
[25]K. Roleder, M. Maglione, M. D. Fontana, and J. Dec, J. Phys.: Condens. Matter **8**, 10669 (1996).
[26]T. Ostapchuk, J. Petzelt, V. Zelezny, S. Kamba, V. Bovtun, V. Porokhonskyy, A. Pashkin, P. Kuzel, M. D. Glinchuk, I. P. Bykov, B. Gorshunov, and M. Dressel, J. Phys.: Condens. Matter **13**, 2677 (2001).
[27]S. Aoyagi, Y. Kuroiwa, A. Sawada, H. Tanaka, J. Harada, E. Nishibori, M. Takata, and M. Sakata, J. Phys. Soc. Jpn. **71**, 2353 (2002).
[28]J. Dec, K. Roleder, and K. Stróż, Solid State Commun. **99**, 157 (1996).
[29]J. H. Kim, J.-Y. Choi, M.-S. Jeong, J.-H. Ko, M. Ahart, Y. H. Ko, and K. J. Kim, J. Korean Phys. Soc. **60**, 1419 (2012).
[30]M. A. Geday and A. M. Glazer, J. Phys. Condens. Matter **16**, 3303 (2004).
[31]R. Vacher and L. Boyer, Phys. Rev. B **6**, 639 (1972).
[32]J. Baedi, S. M. Hosseini, A. Kompany, and E. A. Kakhki, Phys. Stat. Sol. (b) **245**, 2575 (2008).
[33]R. D. King-Smith and D. Vanderbilt, Phys. Rev. B **49**, 5828 (1994).
[34]A. Y. Wu and R. J. Sladek, Phys. Rev. B **27**, 2089 (1983).
[35]J.-H. Ko, S. Kojima, T.-Y. Koo, J. H. Jung, C. J. Won, and N. J. Hur, Appl. Phys. Lett. **93**, 102905 (2008).
[36]J.-H. Ko, T. H. Kim, K. Roleder, D. Rytz, and S. Kojima, Phys. Rev. B **84**, 094123 (2011).
[37]J.-H. Ko, T. H. Kim, S. Kojima, K. Roleder, D. Rytz, C. J. Won, N. J. Hur, J. H. Jung, T.-Y. Koo, S. B. Kim, and K. Park, Curr. Appl. Phys. **12**, 1185 (2012).
[38]A. Bussmann-Holder, H. Beige, and G. Volkel, Phys. Rev. B **79**, 184111 (2009).
[39]K. Szot, W. Speier, G. Bihlmayer, and R. Waser, Nat. Mater. **5**, 312 (2006).
[40]C. L. Jia, A. Thust, and K. Urban, Phys. Rev. Lett. **95**, 225506 (2005).
[41]N. Zhang, H. Yokota, A. M. Glazer, and P. A. Thomas, Acta Cryst. B **67**, 461 (2011).